JPET Fast Forward. Published on December 8, 2005 as DOI: 10.1124/jpet.105.096958

Title Page

Vascular adhesion protein-1 plays an important role in post-ischemic inflammation and neuropathology in diabetic, estrogen-treated ovariectomized female rats subjected to transient forebrain ischemia.

Hao-Liang Xu, Luisa Salter-Cid, Matthew D. Linnik, Eric Y. Wang, Chanannait Paisansathan, and Dale A. Pelligrino

Neuroanesthesia Research Laboratory, Univ. of Illinois at Chicago, Chicago, IL (HX, CP, DAP)

LaJolla Pharmaceutical Company, San Diego, CA (LS, MDL, EYW)

Running Title Page

Running Title: Cerebral ischemia and VAP-1

Corresponding author:

Dale A. Pelligrino, PhD; Professor & Director, Neuroanesthesia Research Laboratory; Univ. of Illinois at Chicago; Molecular Biology Research Building, Room 4320; 900 S. Ashland Avenue; Chicago, IL 60607 ; phone: (312) 355-1666 ; FAX: (815) 333-1493 ; e-mail: dpell@uic.edu

Tables: 1

Figures: 8

References: 40

Words Abstract: 248

Words Introduction: 675

Words Discussion: 1,497

Abbreviations: SSAO, semicarbazide-sensitive amine oxidase; VAP-1, vascular adhesion protein-1; OVX, ovariectomized; TFI, transient forebrain ischemia; ERT, estrogen replacement therapy; STZ, streptozotocin; E_2, 17β-estradiol; CBF, cerebral blood flow; MPO, myeloperoxidase; FJ, Fluoro-Jade; H&E, hemotoxylin & eosin; MAO, monoamine oxidase; DPO, 2,5-diphenyloxdazole; MMP, matrix metalloproteinase; COX, cyclooxygenase; SD, standard deviation; PKC, protein kinase C; PMNL, polymorphonuclear leukocyte.

Recommended Section: Inflammation & Immunopharmacology

JPET Fast Forward. Published on December 8, 2005 as DOI: 10.1124/jpet.105.096958
This article has not been copyedited and formatted. The final version may differ from this version.

Abstract

Endothelial vascular adhesion protein-1 (VAP-1) facilitates leukocyte adhesion and infiltration. This relates partly to the function of VAP-1 as a semicarbazide-sensitive amine oxidase (SSAO). We examined the effects of VAP-1/SSAO inhibition (via LJP-1207) on pial venular leukocyte adhesion and infiltration (at 2-10h reperfusion) and neuropathology (at 72h reperfusion) following transient forebrain ischemia (TFI). A model associated with increased post-ischemic inflammation was used—i.e., diabetic ovariectomized (OVX) female rats given chronic estrogen replacement therapy (ERT). We compared rats treated, either at the onset or at 6h reperfusion, with saline or LJP-1207. Additional rats, rendered neutropenic 24h prior to TFI, were studied. In saline-treated controls, intravascular accumulation of adherent leukocytes gradually increased, reaching 15-20% of the venular area, at which point neutrophil infiltration commenced (at ~6h). In the rats given LJP-1207 at the onset of reperfusion, limited neutrophil adhesion (~5% maximum), and no infiltration, was observed. These results generally paralleled those in neutropenic rats. In rats treated at 6h reperfusion, the pattern of neutrophil adhesion was similar to that of the saline-treated group up to 6h, but further infiltration was essentially prevented. Neurologic outcomes and histopathology were similar to one another in the LJP-1207-treated and neutropenic groups and significantly improved over saline-treated controls. Thus, VAP-1-mediated post-TFI leukocyte adhesion/infiltration, in diabetic OVX females given chronic ERT, contributes substantially to neuropathology. One implication is that specifically preventing leukocyte *infiltration* provides a substantial measure of neuroprotection. This could explain the finding of LJP-1207 having at least a 6-hour therapeutic window, in this model.

Introduction

Post-ischemic neuropathology has been linked to the increases in cerebral vascular leukocyte adhesion and infiltration that often occur following an ischemic event (reviewed by Frijns and Kappelle, 2002). Nevertheless, experimental evidence exists to challenge this view (reviewed by Emerich et al., 2002). Furthermore, recent clinical trials have failed to demonstrate any benefit from treatment with an adhesion molecule antibodies or blockers (see Sughrue et al., 2004). However, these clinical findings are confounded by factors related to immunogenicity (use of non-human antibodies) and inconsistencies in patient recruitment criteria.

A general implication one might derive from these mixed experimental findings is that, while increased leukocyte activity may accompany most cerebral ischemia episodes (especially those with reperfusion), it may not necessarily be a primary contributor to neuropathology in all cases. Results from our laboratory suggest that whether leukocytes contribute to ischemic neuropathology, or not, depends on whether leukocyte (principally neutrophil, Arumugam et al., 2005) infiltration, and not simply venular adhesion, has occurred during the initial 10-12h of reperfusion. Thus, the extent of neuropathology assessed after several days of reperfusion (Santizo et al., 2002) seemed to parallel the patterns of acute neutrophil extravasation (over 10h reperfusion), as viewed in pial venules in situ (Xu et al., 2004). It is relevant to note that these experiments were performed on diabetic, intact, ovariectomized (OVX), and estrogen-treated OVX females in order to test the hypothesis that chronic estrogen replacement therapy is associated with a potentiation of post-ischemic inflammation and neuropathology, opposite to what was previously observed in non-diabetic females (Santizo et al., 2000b). These observations may be of particular interest to post-menopausal females, since women in this age group not only are at greater risk for cerebral ischemic events,

they also often experience an increased incidence of reduced glucose tolerance and hyperglycemia, although not necessarily related to estrogen depletion, per se. Furthermore, recent clinical findings failed to demonstrate any cardiovascular or brain-protective effects of chronic estrogen replacement therapy in post-menopausal women, contrary to results obtained in experimental animals. Therefore, studies employing clinically relevant experimental models associated with a loss of estrogen's neuro- and vasculo-protective effects are important, insofar as they may yield clues that can be used in devising estrogen replacement strategies that will be beneficial.

In the present investigation, we sought to establish a link between the increased post-ischemic leukocyte infiltration ***and*** neuropathology we observed in our earlier studies in diabetic OVX females given chronic estrogen replacement therapy. To that end, we targeted vascular adhesion protein-1 (VAP-1). This protein was identified as playing an important role in promoting leukocyte adhesion as well as transmigration. Those actions of VAP-1 may relate to its direct function as an adhesin, in addition to its enzymatic function as a semicarbazide-sensitive amine oxidase (SSAO) (Salmi et al., 1993;Stolen et al., 2005). In addition to a soluble form found in the blood, VAP-1/SSAO is concentrated in vascular tissue, including cerebral microvessels and endothelial cells (Salmi et al., 1993) and is mobilized to the luminal surface of endothelial cells in the face of an "inflammatory stimulus". However, no studies have addressed whether VAP-1/SSAO influences post-ischemic leukocyte trafficking in the brain. In this study, using diabetic, estrogen-treated OVX females subjected to transient forebrain ischemia (TFI), we examined the role of VAP-1/SSAO in: 1) neutrophil adhesion and infiltration during the initial 10h reperfusion; and 2) the level of neuropathology at 72h reperfusion. Thus, rats were studied in the absence and presence of a novel, highly-selective VAP-1/SSAO inhibitor, LJP-1207 (Salter-Cid et al., 2005). To confirm the importance of neutrophils, rats rendered neutropenic 24h prior to ischemia were also studied. It was

found that, when the VAP-1/SSAO inhibitor was given at the onset of reperfusion, similar to findings in neutropenic rats, neutrophil adhesion was substantially reduced and infiltration, which normally appears after ~6h post-ischemia in these rats, was not observed. When the inhibitor treatment was delayed until 6h reperfusion, infiltration, but not intravascular adhesion, was markedly attenuated relative to saline-treated controls. Irrespective of treatment timing, significant neuroprotection was seen in the presence of the VAP-1/SSAO blocker as well as in neutropenic rats.

Materials and Methods

Animal: The study protocol was approved by the Institutional Animal Care and Use Committee. Ovariectomized (OVX), female Sprague-Dawley rats (200-250 g at arrival) were used. Ovariectomies were performed by the vendor (Charles River) one week prior to shipment. Diabetes was induced via streptozotocin (STZ; 60 mg/kg, iv) at ~1 week following arrival, and the rats were studied ~6-8 weeks later. At 1 week prior to study, 17β- estradiol (E_2) treatment was initiated (0.1 mg/kg/day, ip, for 7 days). Previous work from our laboratory demonstrated that the 0.1 mg/kg daily dose of E_2 results in an average daily plasma E_2 concentration that falls between the peak and nadir levels observed over the normal rat estrous cycle (Xu et al., 2004).

Ischemia model. Right forebrain ischemia was produced by clamping the right common carotid artery, combined with blood withdrawal from the subclavian vein, to decrease cortical cerebral blood flow to 20% of baseline, as measured by laser-Doppler flowmetry. Reperfusion was established, after 20 minutes, via removal of the carotid clamp and reinfusion of withdrawn blood over a 15 min period. The exact procedure employed, with respect to anesthesia, muscle relaxation, and surgical preparation, depended upon whether the animals were to be used in leukocyte

adhesion/infiltration evaluations or long-term recovery and neuropathologic assessments (see below). Results from pilot and published (Wang et al., 1999) investigations established that intra-ischemic CBF relationships between the cortex and subcortical structures did not vary with hormone or glycemic status. Furthermore, cortical CBF recovered to pre-ischemic levels within 2 min following onset of reperfusion and remained within 80% of that level for as long as monitoring continued (up to 4 hours). In preliminary evaluations, we did not observe any differences in post-ischemic CBF recovery when comparing selected rats from each group (see below).

Experimental groups: The studies were organized into two major experimental series. In the first series, pial venular leukocyte adhesion was monitored over the initial 10h reperfusion period. In the second series, post-ischemic neuropathology was assessed in rats exposed to 72h reperfusion. For leukocyte adhesion evaluations, rats were prepared with closed cranial windows 24h prior to study. The procedure for "chronic" placement of cranial windows was described in a previous paper from our laboratory (Xu et al., 2001). Each series was further divided into 4 subgroups. Subgroup 1 received 30 mg/kg iv of the VAP-1/SSAO inhibitor, LJP-1207, at the onset of reperfusion. In subgroup 2, LJP-1207 treatment was given at 6h reperfusion. The third subgroup was a vehicle (saline)-injected control. Subgroup 4 rats were rendered neutropenic prior to ischemia. For these experiments, rats were injected iv with 0.3 ml of a rabbit anti-rat PMNL antibody (from Research Diagnostics, Inc., Flanders, NJ, diluted 1:1) 24h prior to ischemia. In some control and neutropenic rats (3-4 each), arterial blood samples were obtained prior to ischemia and leukocyte composition was examined using hemocytometry.

Leukocyte adhesion/infiltration assessments: In series 1 experiments, on the day of study, the rats were anesthetized with halothane. Paralysis was then induced with curare, followed by tracheotomy and mechanical ventilation. During surgery, anesthesia was maintained with 1.2%

isoflurane / 70% N_2O / 30% O_2. The femoral arteries and veins were cannulated for blood sampling, arterial pressure monitoring, and drug infusions. Rectal temperature was servo-controlled at 37 °C with a heating pad. The right common carotid artery was isolated, followed by insertion of a right subclavian venous catheter. The previously-implanted cranial window was then re-exposed. After the surgery, the isoflurane was discontinued and the rat was maintained on 70% N_2O / 30% O_2-fentanyl (25 μg/kg/h *iv*) thereafter. The space under the window was filled with artificial cerebrospinal fluid (aCSF) that was equilibrated with 10% O_2/ 5%CO_2 with balance of N_2. The 37 °C aCSF was suffused at 0.5 ml/min. A 0.8 mm diameter laser-Doppler flow probe (Perimed, Jarfälla, Sweden) was secured to the cranial window above the right parietal cortex and baseline measurements, in perfusion units, were recorded. The leukocyte activity of pial venules was monitored using a rhodamine-filtered digital video camera (Photometrics, Fryer Co. Inc., Huntley, IL), attached to a microscope. Leukocytes were labeled with rhodamine 6G (200 μg/ml in 0.9% saline). The rhodamine was given initially as an IV bolus (l ml), and followed by continuous infusion at a rate of l ml/hr (Santizo et al., 2000b). Images of leukocytes were captured and saved, using the MetaMorph software system (Universal Imaging Corp., Downingtown, PA), and displayed on a computer monitor. Leukocyte dynamics were monitored after 2, 4, 6, 8, and 10 h of reperfusion. Illumination was limited to <60 seconds at a time to avoid photoquenching. Leukocyte adherence was measured in all experiments as the area percentage of leukocytes overlapping the viewed venular area. The *viewed venular area* was determined from frames captured following switching from fluorescence to standard light microscopy. The value of the *viewed venular area* was expressed as a percentage of the total area exposed in the captured frame. Expressing leukocyte adherence (and infiltration—see below) as a fractional area, rather than the *number* of rhodamine-positive cells per unit venular area was necessitated by the two-dimensional view generated by our

video/microscopy system. Thus, we could not readily distinguish overlapping firmly adherent (or extravasated) cells from one another. Such overlap became increasingly prominent with time in a number of instances. In many of the saline-treated controls (i.e., non-LJP-1207-treated; non-neutropenic), leukocyte infiltration was seen (but only at time points >6h). When extravasation was observed, another measurement strategy was applied. Thus, in addition to the measurement of leukocyte adherence described above, the total area of rhodamine-positive cells was counted, including cells that were distinctly extravascular. In both instances, the denominator was *viewed venular area*. An additional calculation was then made, where the percentage of "adherent" leukocytes was subtracted from the total leukocyte percentage. The result provided us with an "index of infiltration". It should be noted that in rats from the above diabetic groups not rendered ischemic, but where pial venular leukocytes were monitored over 10-12h (sham ischemic time controls—data not shown), the level of leukocyte adhesion remained low throughout the monitoring period. In some of the rats from each group, at the termination of the study, brains were harvested for immunohistochemical analysis of myeloperoxidase (MPO) expression and histopathologic analysis via Fluoro-Jade (see below). This was done primarily to evaluate whether leukocyte (neutrophil) extravasation was present in "non-window" brain structures (i.e., cortex, striatum, hippocampus, thalamus) where ischemic damage has been shown to occur in diabetic E_2-treated OVX females (Santizo et al., 2002); ***and*** whether any signs of neuronal damage were evident. Preparation of 7 μm-thick paraffin-embedded coronal sections for MPO immunohistochemistry was described in an earlier publication (Santizo et al., 2000a).

Neuropathology assessments: For series 2 studies (72h reperfusion), the rats were prepared for induction of transient forebrain ischemia, as described above. However, in this instance, the rats were intubated endotracheally and the short-acting muscle relaxant, vecuronium bromide, was given as an

iv infusion to maintain paralysis. An area of the skull overlying the right parietal cortex was thinned to translucency with a drill, and an inverted 21G needle was glued in place over the bone "window". This was used as a guide for a 0.8 mm diameter laser-Doppler flow probe. Following preparation, the rats were switched to fentanyl/N_2O (see above). Both scalp and rectal temperatures were maintained at 37°C. At the end of the 20 min ischemia period (see above), the carotid clamp was removed and the withdrawn blood was reinfused. The catheters were removed and the skin over all wound sites was infiltrated with bupivacaine and sutured. Muscle relaxation, then anesthesia, was discontinued. When spontaneous breathing was re-established, the rats were extubated, and returned to their cages. Neurologic function assessments were performed at 24, 48, and 72h post-ischemia (details are provided below). At 72h post-ischemia, the brains were prepared for histopathologic examination according to procedures described in earlier publications (Santizo et al., 2000a;Wang et al., 1999). 7 µm coronal sections, at the level of the striatum and hippocampus (~1 and 4 mm posterior to the bregma, respectively), were obtained and stained with Fluoro-Jade B (FJ), according to instructions provided by the supplier (Histo-Chem Inc., Jefferson, AR). Fluoro-Jade reactivity has been used by other investigators to identify degenerating neurons (Schmued and Hopkins, 2000). Sections were viewed through a fluorescent microscope (Nikon), and a series of images were captured from the cortex, striatum, hippocampus, and thalamus, using a Spot 2 digital camera and the MetaMorph program. The number of FJ-positive neurons were counted using the Image Pro Plus system (Media Cybernetics, Silver Spring, MD). In some rats of the present study, two adjacent (or nearly adjacent) 7 µm sections were prepared with FJ- or hemotoxylin and eosin (H&E)-staining (see Santizo et al., 2002). Photomicrographs were then obtained and compared.

For neurologic function assessments, as described in greater detail in previous reports from our laboratory (Wang et al., 1999), a blinded observer scored the rats each day for 3 days. There

JPET Fast Forward. Published on December 8, 2005 as DOI: 10.1124/jpet.105.096958
This article has not been copyedited and formatted. The final version may differ from this version.

were 6 different categories, with some emphasis placed on motor function: ***(i)*** consciousness, where scores range from 0 (normal) to 4 (seizures); ***(ii)*** rope platform (ranges from 0 [climbs to platform] to 4 [no grasp reflex]); ***(iii)*** limb tone (normal=0, weak=1); ***(iv)*** walking (ranges from 0 [normal] to 4 [unable to stand]); ***(v)*** rotating screen, where the range is 0 (grasps to 180° > 5 sec) to 3 (falls from vertical screen); and ***(vi)*** pain reflex (normal=0, hypoactive=1). A summed daily score of 0 would indicate no dysfunction. Rats that did not regain consciousness following ischemia or failed to survive at least 48h post-ischemia were not counted. If a rat died between 48 and 72h reperfusion, the 3rd-day score was extrapolated from the average scores from days one and two. All rats surviving the full 3 days were anesthetized with isoflurane and subjected to perfusion fixation of the brain. The brains were subsequently removed and processed for histologic examination.

Analyses of LJP-1207 selectivity, efficacy, and pharmacokinetics: LJP 1207 [N'-(2-phenyl-allyl)-hydrazine hydrochloride; formula weight of 184.6], which, by virtue of a hydrazino functional group, is a potent, selective inhibitor of VAP-1/SSAO enzymatic activity. That selectivity was established in pilot studies, where LJP 1207 was screened for potential cross-reactivity with a variety of enzymes. Rat VAP-1/SSAO activity was measured in rat lung homogenates using a radiochemical assay (Lizcano et al., 1998). Briefly, the tissue was homogenized 1:20 (w/v) in 10 mM PBS and centrifuged at 1000g for 10 minutes at 4°C. VAP-1/SSAO activity in 100 µl of the supernatant was determined using 20 µM ^{14}C- benzylamine as substrate and, when appropriate, added LJP-1207. The reaction was carried out at 37° C in a final volume of 400 µl of 100 mM potassium phosphate buffer (pH 7.2) and stopped with 100 µl of 2 M citric acid. Radioactively labeled products were extracted into toluene/ethyl acetate (1:1, v/v) containing 0.6% (w/v) 2,5-diphenyloxdazole (DPO) before liquid scintillation counting. All experiments were performed in the presence of 1 µM clorgyline and pargyline to inhibit MAO-A

and MAO-B activities, respectively. Inhibition was calculated as percent inhibition compared to saline-treated control after correcting for background absorbance, and IC_{50} values were calculated using GraphPad Prism software.

Monoamine oxidase (MAO)-A and MAO-B activities were measured using a coupled colorimetric method (Holt et al., 1997). Recombinant human MAO-A and human MAO-B enzymes were obtained from BD Biosciences (Bedford, MA). The assay was performed in 96-well microtiter plates as follows. A pre-determined amount of inhibitor diluted in 0.2 M potassium phosphate buffer, pH 7.6, was added to each well of a 96 well microtitre plates. The final concentration of inhibitor was between 50 nM and 1 mM. Controls lacked inhibitor. The following agents were then added to a final reaction volume of 200 µl in 0.2 M potassium phosphate buffer, pH 7.6: 0.04 mg/ml of MAO-A or 0.07 mg/ml MAO-B enzyme, 15 µl of 10 mM tyramine substrate (for MAO-A), or 15 µl 100 mM benzylamine substrate (for MAO-B), and 50 µl of freshly made chromogenic solution containing 750 nM vanillic acid (Sigma), 400 nM 4-aminoantipyrine (Sigma) and 12 U/ml horseradish peroxidase (Sigma). The plates were incubated for 1 hr at 37°C and the increase in absorbance, reflecting MAO activity, was measured at 490 nm using a microplate spectrophotometer (Power Wave 40, Bio-Tek Inst.). Clorgyline (0.5 µM) and pargyline (10 µM), inhibitors of MAO-A and –B, respectively, were added to some wells as positive controls for MAO inhibition. The level of inhibition was calculated as percent inhibition compared to control after correcting for background absorbance, and IC_{50} values were calculated using GraphPad Prism software. The inhibitory effects of LJP-1207 toward cyclooxygenase (COX)-1, COX-2, matrix metalloproteinase-9 (MMP9), protein kinase C (PKC), caspase 3, cathepsin G, and xanthine oxidase were assayed by MDS Pharma Services (Taipei, Taiwan). The methodologic references can be found at *http://discovery.mdsps.com/Catalog/*. With the exception of COX-1

JPET Fast Forward. Published on December 8, 2005 as DOI: 10.1124/jpet.105.096958
This article has not been copyedited and formatted. The final version may differ from this version.

(IC_{50}=3 μM), the IC_{50} values of LJP-1207 toward the remaining enzymes exceeded 10 μM. In separate assays, we evaluated the level of VAP-1/SSAO inhibition at 6h following iv administration of LJP-1207 or saline in non-ischemic, diabetic, E_2-treated OVX females (n=6, each group). Samples of lung and pial tissue were obtained in each animal. Enzyme activities in lung tissue samples were measured in each animal, whereas the pial samples were pooled, according to treatment group, prior to the radiochemical assay (Lizcano et al., 1998). For this assay, 100μl of sample (diluted 1:20, w/v, in PBS) were used in each reaction. The backgrounds were determined by pre-inhibition of each sample with 1mM semicarbazine, 1μM pargyline, and 1μM clorgyline for 30min.

Plasma pharmacokinetics of LJP-1207 were determined in 3 rats by a contract research service company (Cerep, Redmond, WA). One mg/kg of LJP-1207 was injected intravenously. Blood was obtained from a jugular vein catheter at 5, 15, 60, 120, 240, 360, and 1440 min. Aliquots were collected in tubes coated with lithium heparin and plasma was harvested and kept frozen at -20 °C until analysis. Samples were processed using acetonitrile precipitation and analyzed by HPLC-MS/MS. The data were used to generate concentration vs time curves and allow the determination of fundamental pharmacokinetic data (e.g., Cmax, Tmax, AUC, clearance, terminal elimination half-life, oral bioavailability, and volume of distribution) using WinNonlin software.

Statistics: For parametric data, statistical analyses were performed using paired t-test and one-way ANOVA with a post hoc Tukey test for multiple comparison procedures. For non-parametric data analysis (neurologic outcomes), we used a one-way ANOVA on ranks, with post-hoc analysis via Dunn's method. A level of $P<0.05$ was considered significant in all statistical tests. Values are presented as mean ± SD. All drugs/chemicals were obtained from Sigma, unless otherwise stated.

JPET Fast Forward. Published on December 8, 2005 as DOI: 10.1124/jpet.105.096958
This article has not been copyedited and formatted. The final version may differ from this version.

Results

LJP-1207 pharmacology. The IC_{50} values of LJP-1207 toward VAP-1/SSAO, MAO-A, and MAO-B, measured in purified enzyme or homogenized tissue preparations, are provided in Table 1. Thus, LJP-1207 displayed a 10^3-10^4 times greater potency toward VAP-1/SSAO compared to the other amine oxidases. The choice of the 30 mg/kg dose of LJP 1207 used in the present study was guided by evaluation of its plasma pharmacokinetics, the selectivity data provided in Table 1 (as well as the data provided by MDS Pharma Services—see Materials and Methods section), and measurements of SSAO activity in lung and pial tissue at 6h following iv injection. The elimination half-life of LJP 1207 following a 1 mg/kg iv administration was 183 minutes with a clearance of 97 mL/min/kg (n=3). The maximum concentration observed at the first time point, 5 minutes after injection, was 292 ng/mL. A linear extrapolation of the 1 mg/kg pharmacokinetic data results in an estimated peak plasma level of LJP-1207 of approximately 30 μM at the 30 mg/kg dose. At 6h post-LJP-1207 administration the relative levels of VAP-1/SSAO activity in lung tissue harvested from E_2-treated OVX females were significantly decreased to 31±4 % of the level measured in saline-injected rats (n=6). In the pooled pial samples, VAP-1/SSAO activity in the LJP-1207-treated rats was 40% lower than that seen in the saline-treated animals. These data indicate that although there is substantial exposure to LJP-1207 at the doses employed in this study, the concentrations of LJP-1207 achieved in the circulation, at 6 hr post-treatment, remain well within the drug's selectivity range. The apparently lower magnitude reduction in VAP-1/SSAO activity in

pial vs lung tissue may reflect some blood-brain barrier impediment to drug passage into cerebral vascular cells. However, since the pial tissue used in these assays was not obtained from rats exposed to ischemia and reperfusion, it is likely that the level of VAP-1/SSAO inhibition measured in these samples is of a lesser magnitude than one might observe in the post-ischemic reperfusion period. That is, some diminished blood-brain barrier function can be anticipated post-ischemically, thereby allowing passage of more drug into the brain and cerebral vascular cells.

Arterial blood variables. Arterial PCO_2 and PO_2 measurements obtained prior to 20 min of ischemia, at the end of ischemia, and during 10h reperfusion (series 1) remained between 32-38 mmHg and above 100 mmHg, respectively, during the entire study. As commonly seen with this model (see Xu et al., 2004), end-ischemic arterial pH was significantly lower than the pre-ischemic value in all experimental groups (mean [± SD] end-ischemic vs pre-ischemic values for all groups were 7.39 ± 0.02 vs 7.48 ± 0.02, respectively). Pre-ischemic MABP values were similar among groups, and were reduced, during ischemia, to 28-32 mmHg. Plasma glucose values, in samples obtained immediately prior to ischemic onset, were 27.6 ± 1.4, 27.2 ± 2.0, 26.3 ± 2.8, and 28.1 ± 4.2 mM in the saline-treated, LJP-1207-0, LJP-1207-6, and neutropenic groups, respectively. In rats subjected to 20 min ischemia and 72h reperfusion (series 2), peri-ischemic arterial PCO_2, PO_2, pH, and MABP showed variations similar to those seen in series 1 experiments; and plasma glucose values were 27.0 ± 3.7, 26.0 ± 7.4, 30.3 ± 5.1, and 27.8 ± 6.5 mM in the saline-treated, LJP-1207-0, LJP-1207-6, and neutropenic groups, respectively.

Post-ischemic leukocyte adhesion. In saline-treated control E_2-treated diabetic OVX females, leukocyte adhesion showed a progressive increase between 2 and 6 h reperfusion (fig. 1A). The majority of these rats (4 of 7) displayed an extravascular presence of leukocytes beginning around the 6 h time point of reperfusion (fig. 2). By 10h reperfusion, 6 of the 7 rats in the saline-treated

group exhibited extravasated leukocytes. Quantitatively, that is reflected by higher values for total leukocyte presence (fig. 1B) vs leukocytes in contact with cerebral venules (fig. 1A). This is illustrated in fig. 1C, where the calculated differences between total and adherent leukocytes are summarized. Only the 6-10h reperfusion values for the saline and 6h treatment groups are displayed in fig. 1C, since only rats from those groups exhibited any detectable extravascular leukocyte presence during that time period. On the other hand, in rats treated with the VAP-1/SSAO inhibitor, LJP-1207, at the onset of reperfusion (0h), leukocyte adhesion remained significantly below the levels observed in the saline- and the 6h-treatment groups throughout the 10h reperfusion period. Furthermore, no signs of extravasation were seen in this group (fig. 2), as reflected in identical values when comparing leukocyte adhesion (fig. 1A) to total leukocyte presence (fig. 1B). In rats where LJP-1207 treatment was given at 6h reperfusion, the temporal pattern of post-ischemic leukocyte adhesion tracked that of the saline-treated control group out to 6h (fig. 1A; fig. 2). Also, in 3 of the 8 rats studied in the 6h treatment group, a slight degree of leukocyte infiltration was seen at 6h reperfusion and thereafter; although comparisons of total leukocyte presence (fig. 1B) ***and*** leukocyte adhesion (fig. 1A), at given time points over the 6-10h timeframe, yielded no statistically significant differences. Treatment of the rats with the anti-PMNL antibody was found to be effective in selectively depleting circulating neutrophils. Thus, antibody treatment reduced blood neutrophil content to barely detectable levels (from 4,176 ± 1,796 to 63 ± 210 neutrophils/mm^3), without having any significant effect on lymphocyte content (10,419 ± 3,892 vs 7,043 ± 4,761 lymphocytes/mm^3 in vehicle vs antibody-treated rats, respectively). In the neutropenic rats, far fewer adherent cells were observed over the 10h period of reperfusion (not shown), to the extent that a <3% pial venular occupancy was observed at 6 and 10h (figs. 1A, 1B; $p<0.05$ vs saline-treated control and LJP-1207-6, at all time points). Comparisons between the neutropenic and LJP-1207-0

groups revealed no statistically significant differences. These findings not only support the effectiveness of the anti-PMNL strategy, but also indicate that PMNLs comprise a substantial fraction of the entire mass of adherent blood cells seen during the initial hours of ischemic reperfusion.

Examination of coronal sections prepared from brains harvested at 10-12h reperfusion revealed the presence of extravascular PMNLs (MPO immunoreactivity) in the ischemic hemispheres of saline-treated rats, especially in the cerebral cortex. This was observed both at deep and superficial layers of the cortex (fig. 3). In the LJP-1207-6 group, MPO expression was detected almost exclusively in association with blood vessels (fig. 3). In the LJP-1207-0 and neutropenic (not shown) groups, little or no MPO expression was observed. Thus, at least in the cortex, these findings seem to track what was observed in the intravital microscopy evaluations. However, a rather limited intra- and extravascular MPO immunoreactivity was seen in the ischemic striatum, hippocampus, and thalamus (fig. 3; results for hippocampus not shown)—regions that displayed areas of neuronal damage in saline-treated animals (see Histopathology below).

Neurologic outcomes. The neurologic outcome scores (three day total) for the 4 groups are summarized in figure 4. The non-parametric data is presented as a scatter plot, with median values for each group. Since no significant differences were observed when comparing saline-treated rats run in parallel with the two LJP-1207-treated and the anti-PMNL-treated groups, the data from all control groups were combined. A significantly greater neurologic impairment was noted when comparing the control to the LJP-1207-0, LJP-1207-6, and neutropenic groups (median scores of 19, 2, 4, and 4, respectively).

Histopathology. As a general observation, FJ-staining of brain sections in saline-treated control rats revealed damage in the medial thalamus and scattered throughout the cortex, in addition to the

hippocampus and dorsolateral striatum. These results are consistent with published information derived from studies on hyperglycemic rats subjected to TFI (Ding et al., 2004;He et al., 2003;Li et al., 1998a;Li et al., 1998b). Far fewer numbers of degenerating (i.e., FJ-positive) cells were observed in the LJP-1207-treated and neutropenic groups (fig. 5). In several rats from each group, brains were obtained for Fluoro-Jade analysis following the 10-12h period of leukocyte monitoring. No FJ reactivity was detected in any of these animals (not shown). Thus, neuronal damage appears to occur well after the onset of neutrophil extravasation, making it highly unlikely that neutrophils played any sort of "bystander" role (Emerich et al., 2002). Examples of the patterns of brain cell damage seen in the saline- and the two LJP-1207-treated groups are presented in figures 6-7. The neutropenic group is not represented since these rats exhibited relatively few FJ-positive cells (similar to the rats treated with LJP-1207 at the onset of reperfusion). The pattern seen in the saline-treated group is similar to that reported in an earlier publication from our laboratory (Santizo et al., 2002). It should be mentioned that almost no FJ-positive cells were observed in the non-ischemic left hemisphere in any animal. These figures also include higher magnification views in the cortex, striatum, and thalamus. The higher magnification view revealed that the FJ-positive cells had the appearance of neurons. In saline-treated controls, the greatest numbers of degenerating neurons were seen in the cortex and striatum (fig. 6A, 6D). In fact, all 10 control rats evaluated showed damage in these two regions. The presence of neurodegeneration in the thalamus was detected in 80% of the saline-treated controls (fig. 7A); while hippocampal damage was seen in 70% of the controls (fig. 7D). In the hippocampus, hilar (CA4) damage was the most frequently-observed pathology. FJ-positive CA4 pyramidal cells were sometimes accompanied by the presence of FJ-reactive cells in the CA1 region (not shown) and the dentate. In contrast, in the rats treated with the VAP-1/SSAO inhibitor at the onset of reperfusion, no hippocampal damage was observed (fig. 7E),

and only a few isolated degenerating neurons were observed in the cortex (fig. 6B), striatum (fig. 6E) and thalamus (fig. 7B). In rats treated with LJP-1207 at 6h of reperfusion, significantly fewer FJ-positive neurons were observed in the above regions relative to saline-treated controls. When comparing the two treated groups, a significantly greater number of FJ-positive cells were seen in the cortex of the 6h-treatment group (fig. 5; fig. 6C); and two of the six 6h rats (fig. 7F) showed degenerating neurons in the CA4 (but none in the CA1 or dentate). To provide a measure of validation for the FJ results, we compared adjacent coronal sections, where one section was FJ-stained and the other was stained with H&E. We found very good agreement in representative brain section comparisons. This was seen in cortical, striatal, hippocampal, and thalamic views. Three examples are provided in figure 8. The first is taken at the level of the dentate/hilar region of the hippocampus in a saline-treated rat (fig. 8A, 8B). The second is taken from the same region in a 6h LJP-1207-treated (fig. 8C, 8D) rat. The third example is from the cerebral cortex of a saline-treated control rat (fig. 8E, 8F). In fig. 8A-D, one should particularly note the distinction between the dorsal and ventral aspects of the dentate. That is, the pyknotic-appearing granule cells of the ventral aspect (fig. 8B) display a substantial FJ reactivity (fig. 8A), as opposed to the normal-appearing granule cells of the dorsal dentate, which show little or no FJ reactivity. In contrast, in the H&E-stained section obtained from the 6h LJP-1207-treated rats, the dentate granule cells appear to be undamaged (fig. 8D). No FJ-reactivity was observed in those cells (fig. 8C). Moreover, the transition from normal-appearing to pyknotic hilar neurons seen in the H&E-stained sections (fig. 8B, 8D) was reflected in the pattern of FJ-staining (fig. 8A, 8C).

Discussion

There were several key findings in this study. First, in agreement with a recent report from our laboratory (Xu et al., 2004), chronic E_2 replacement therapy in diabetic OVX female rats was associated with substantial time-dependent increases in cerebral leukocyte adhesion, over the initial 6h of reperfusion following forebrain ischemia. Subsequently, neutrophil infiltration was observed. Second, inhibition of VAP-1/SSAO at the onset of reperfusion, as well as pre-ischemic neutrophil depletion, resulted in marked reductions in leukocyte adhesion and an absence of neutrophil infiltration. Third, delaying inhibitor treatment until 6h reperfusion prevented infiltration without affecting the initial (i.e., 0-6h) pattern of neutrophil adhesion. Fourth, both VAP-1/SSAO inhibition protocols ***and*** neutropenia were associated with significantly less neuropathology compared to saline-treated controls. Thus, with respect to interventions that restrict post-ischemic neutrophil infiltration in E_2-treated diabetic OVX female rats subjected to forebrain ischemia, a therapeutic window of at least 6h appears to be present.

We used Fluoro-Jade staining to identify histopathology. Previous studies have shown excellent agreement when comparing Fluoro-Jade to other accepted techniques for identifying neuronal damage or loss in the brain in neuropathology models (Anderson et al., 2005;Bendel et al., 2005;Kubova et al., 2001;Siman et al., 2005;Wang et al., 2003) (see also fig. 8). One advantage of Fluoro-Jade is that damage is more readily detected in comparison to other commonly-employed techniques. This is exemplified in direct comparisons between sections prepared with Fluoro-Jade and H&E-stained sections (see fig. 8). A potential drawback with Fluoro-Jade is that, under some circumstances, non-neural cells, such as astrocytes, may become Fluoro-Jade-positive. However, evidence indicates that such “extra-neuronal” staining may only be observed following prolonged

recovery periods (i.e., weeks, rather than days, Butler et al., 2002). In the present study, where 3-day recovery periods were utilized, higher magnification views of brain regions displaying Fluoro-Jade reactivity revealed cells with neuronal morphology.

The influence of VAP-1/SSAO on the adhesion-transmigration cascade may occur at multiple sites. Thus, results comparing wild-type and VAP-1/SSAO knockout mice (Stolen et al., 2005), using an in vivo model of cytokine-induced cremaster inflammation, indicated that VAP-1/SSAO may play independent roles in supporting both firm adhesion of leukocytes ***and*** leukocyte transmigration. Such a dual role for VAP-1/SSAO could account for the present findings, where inhibitor treatments applied around the onset of leukocyte infiltration (6h reperfusion, Xu et al., 2004) were associated primarily with preventing diapedesis; while vascular adherence of leukocytes remained at the higher levels seen in the absence of treatment. That is, a restriction of vascular adhesion was not required for LJP-1207 to prevent neutrophil infiltration.

Findings in rodents subjected to transient focal ischemia point to a temporally progressive adhesion and infiltration of leukocytes following restitution of flow, with neutrophils leading the way. Moreover, in many instances, anti-leukocyte strategies were effective in reducing neuropathology (e.g., Frijns and Kappelle, 2002). A limited number of published reports have examined post-ischemic leukocyte contributions in forebrain/global ischemia models. Analysis of results from those studies, in normoglycemic males, is complicated by the fact that a number of different models were used, including several large vessel occlusion models (Abels et al., 2000;Beck et al., 1997;Dirnagl et al., 1994;Hudetz et al., 1999); and cardiac arrest (Bottiger et al., 1998). With the exception of cardiac arrest, post-ischemic leukocyte adhesion was rather modest. In the rats subjected to cardiac arrest and recovery, a significant elevation in myeloperoxidase (MPO) immunoreactive cells (principally neutrophils) were observed in the cortex at 6h and 1 week of

recovery. However, the presence of neutrophils did not correlate well with the injury patterns in other brain regions. In *non*-diabetic female rats, we found an inverse relationship between estrogen and post-ischemic leukocyte adhesion (Santizo et al., 2000b), at least out to 6h reperfusion. In the 6-10h reperfusion interval (HL Xu, DA Pelligrino, unpublished), only untreated OVX females, but not intact and E_2-treated OVX females, exhibited signs of infiltration. On the other hand, in the presence of hyperglycemia, present and published (Lin et al., 2000;Xu et al., 2004) findings indicate an exacerbation of leukocyte trafficking following transient forebrain ischemia. Furthermore, these hyperglycemic animals displayed greater levels of neuropathology (see also Santizo et al., 2002) compared to animals where post-ischemic leukocyte activity was modest.

However, such findings can only be considered as correlative. Indeed, one of the key criticisms raised in opposing a pathogenic role for neutrophils in ischemia/reperfusion models is the absence of evidence showing significant neutrophil trafficking in advance of neuronal damage (Emerich et al., 2002). In fact, in one publication (Ahmed et al., 2000), it was reported that increasing peri-ischemic leukocyte activity, via LPS pretreatment 24h prior to temporary middle cerebral artery occlusion, was associated with *reduced* brain damage. However, LPS pretreatment induces tolerance to ischemia through a variety of mechanisms (Kariko et al., 2004). Thus, the impact of the findings by Ahmed et al. (2000), as it applies to the role of leukocytes in ischemic brain damage, is questionable. In the present study, an increased neutrophil trafficking in advance of brain damage was seen. Moreover, the various interventions designed to specifically impede that process, but at different steps (i.e., neutropenia or early and delayed VAP-1/SSAO-inhibitor administration), were all efficacious in restricting neutrophil *infiltration*, and were all associated with a reduced neuropathology. This is compelling evidence favoring a causative role for neutrophils in the post-ischemic neuronal damage seen in diabetic OVX rats given chronic estrogen

replacement. However, since lymphocytes represent the major white blood cell type in rats and lymphocyte trafficking is regulated by VAP-1/SSAO (Salmi et al., 1993), possible contributions from lymphocytes warrant consideration. Limited evidence to date (focal ischemia/reperfusion only) indicates that lymphocyte infiltration occurs much later (days), compared to neutrophils (Arumugam et al., 2005). Assuming a similar time differential in forebrain ischemia/reperfusion, it appears unlikely that the effects of LJP-1207 observed in the present study relate in any meaningful way to actions toward lymphocytes. One reason is that the half-life for the drug in rats is only 3 hours. It is improbable that sufficient LJP-1207 remains in the circulation 2-3 days following its administration. Another finding favoring a role for neutrophils over lymphocytes relates to the capacity for the anti-PMNL antibody to impart neuroprotection in the absence of any significant effects on lymphocyte numbers.

The processes utilized by neutrophils to mediate brain damage can include release of reactive O_2 species and proteases. Both, but especially the latter, when released into the brain parenchyma can lead to damage of the extracellular matrix and blood-brain barrier (Gidday et al., 2005) and facilitate the appearance of the so-called “hemorrhagic transformation” (Wang et al., 2004).

One confounding observation in the present study relates to the presence of extravascular PMNLs in brain regions exhibiting neuropathology. Thus, the degree of leukocyte infiltration observed after 10h reperfusion when viewing pial venules was mirrored throughout the ischemic cerebral cortex—a region displaying substantial neuronal damage in saline-treated controls. Curiously, in the deeper forebrain structures that typically display post-ischemic neuropathology in association with diabetes and hyperglycemia (i.e., hippocampus, striatum, and thalamus), only a modest presence of PMNLs was observed in brains harvested at 10-12h of reperfusion. These latter

observations do not necessarily obviate contributions from leukocytes to the damage seen in these deeper structures. Since information regarding the 12-72h period of reperfusion is lacking, the possibility remains that leukocyte activity may peak later in those regions in relation to the cortex (see, for example, Bottiger et al., 1998;Lin et al., 2000). Another possibility that merits consideration is that the cortex may represent the proximal site of neuronal damage. This could result in loss of cortical afferent inputs to those other structures and contribute to the subsequent appearance of neuropathology (e.g., Block et al., 2005). Thus, the link between PMNL trafficking ***and*** damage to the other structures might only be indirect. This could explain why anti-PMNL strategies, in the present study, protected both the cortex and the deeper structures as well, despite limited leukocyte activity in the subcortical regions.

In conclusion, chronic E_2 replacement in diabetic OVX females is associated with a pronounced exacerbation of leukocyte adhesion and infiltration following transient forebrain ischemia. The opposite effect is seen in non-diabetics. Those opposing actions of chronic E_2 replacement on leukocytes are paralleled by neuropathologic findings. A similar result, with respect to E_2 replacement *potentiating* post-ischemic leukocyte activity and brain damage in diabetic OVX females, was recently reported for rats subjected to temporary middle cerebral artery occlusion (Yong et al., 2005). The results of the current study also indicated that VAP-1/SSAO is a key component in the inflammatory cascade leading to neutrophil infiltration and subsequent neurotoxicity, in E_2-treated OVX diabetics. The fact that VAP-1/SSAO activity has been reported to be enhanced in diabetics (Yu et al., 2003) may have some relevance in this regard. Finally, gaining an understanding of the mechanisms responsible for this “transformation” of estrogen from a neuroprotective to a neurotoxic agent may provide clues that could help to explain the results of

recently-published clinical trials (reviewed by Brass, 2004) showing a lack of benefit, with respect to stroke, of hormone replacement therapy in post-menopausal females.

Acknowledgements

We wish to acknowledge the expert technical assistance of Susan Anderson, Dennis Riley, Shuhua Ye, Li Huang, and Andrew Miller.

References

Abels C, Rohrich F, Corvin S, Meyermann R, Baethmann A, and Schurer L (2000) Leukocyte-endothelium-interaction in pial vessels following global, cerebral ischaemia. *Acta Neurochir.(Wien.)* **142**:333-339.

Ahmed SH, He YY, Nassief A, Xu J, and Xu XM (2000) Effects of lipopolysaccharide priming on acute ischemic brain injury. *Stroke* **31**:193-199.

Anderson KJ, Miller KM, Fugaccia I, and Scheff SW (2005) Regional distribution of fluoro-jade B staining in the hippocampus following traumatic brain injury. *Exp.Neurol.* **193**:125-130.

Arumugam TV, Granger DN, and Mattson MP (2005) Stroke and T-cells. *Neuromolecular Med.* **7**:229-242.

Beck J, Stummer W, Lehmberg J, Baethmann A, and Uhl E (1997) Leukocyte-endothelium interactions in global cerebral ischemia. *Brain Edema.X.70.* **53-55**.

Bendel O, Bueters T, von Euler M, Ove OS, Sandin J, and von Euler G (2005) Reappearance of hippocampal CA1 neurons after ischemia is associated with recovery of learning and memory. *J.Cereb.Blood Flow Metab* **25**:1586-1595.

Block F, Dihne M, and Loos M (2005) Inflammation in areas of remote changes following focal brain lesion. *Prog.Neurobiol.* **75**:342-365.

Bottiger BW, Schmitz B, Wiessner C, Vogel P, and Hossmann KA (1998) Neuronal stress response and neuronal cell damage after cardiocirculatory arrest in rats. *J.Cereb.Blood Flow Metab.* **18**:1077-1087.

Brass LM (2004) Hormone replacement therapy and stroke: clinical trials review. *Stroke* **35**:2644-2647.

Butler TL, Kassed CA, Sanberg PR, Willing AE, and Pennypacker KR (2002) Neurodegeneration in the rat hippocampus and striatum after middle cerebral artery occlusion. *Brain Res.* **929**:252-260.

Ding C, He Q, and Li PA (2004) Activation of cell death pathway after a brief period of global ischemia in diabetic and non-diabetic animals. *Exp.Neurol.* **188**:421-429.

Dirnagl U, Niwa K, Sixt G, and Villringer A (1994) Cortical hypoperfusion after global forebrain ischemia in rats is not caused by microvascular leukocyte plugging. *Stroke* **25**:1028-1038.

Emerich DF, Dean RL, III, and Bartus RT (2002) The role of leukocytes following cerebral ischemia: pathogenic variable or bystander reaction to emerging infarct? *Exp.Neurol.* **173**:168-181.

Frijns CJ and Kappelle LJ (2002) Inflammatory cell adhesion molecules in ischemic cerebrovascular disease. *Stroke* **33**:2115-2122.

Gidday JM, Gasche YG, Copin JC, Shah AR, Perez RS, Shapiro SD, Chan PH, and Park TS (2005) Leukocyte-derived matrix metalloproteinase-9 mediates blood-brain barrier breakdown and is proinflammatory following transient focal cerebral ischemia. *Am.J.Physiol.* **289**:H558-H568.

He Q, Csiszar K, and Li P (2003) Transient forebrain ischemia induced phosphorylation of cAMP-responsive element-binding protein is suppressed by hyperglycemia. *Neurobiol.Dis.* **12**:25-34.

Holt A, Sharman DF, Baker GB, and Palcic MM (1997) A continuous spectrophotometric assay for monoamine oxidase and related enzymes in tissue homogenates. *Anal.Biochem.* **244**:384-392.

Hudetz AG, Wood JD, and Kampine JP (1999) Nitric oxide synthase inhibitor augments post-ischemic leukocyte adhesion in the cerebral microcirculation in vivo. *Neurol.Res.* **21**:378-384.

Kariko K, Weissman D, and Welsh FA (2004) Inhibition of toll-like receptor and cytokine signaling--a unifying theme in ischemic tolerance. *J.Cereb.Blood Flow Metab* **24**:1288-1304.

Kubova H, Druga R, Lukasiuk K, Suchomelova L, Haugvicova R, Jirmanova I, and Pitkanen A (2001) Status epilepticus causes necrotic damage in the mediodorsal nucleus of the thalamus in immature rats. *J.Neurosci.* **21**:3593-3599.

Li C, Li PA, He QP, Ouyang YB, and Siesjo BK (1998a) Effects of streptozotocin-induced hyperglycemia on brain damage following transient ischemia. *Neurobiol.Disease.* **5**:117-128.

Li PA, Vogel J, He QP, Smith ML, Kuschinsky W, and Siesjo BK (1998b) Preischemic hyperglycemia leads to rapidly developing brain damage with no change in capillary patency. *Brain Res.* **782**:175-183.

Lin B, Ginsberg MD, Busto R, and Li L (2000) Hyperglycemia triggers massive neutrophil deposition in brain following transient ischemia in rats. *Neurosci.Lett.* **278**:1-4.

Lizcano JM, Tipton KF, and Unzeta M (1998) Purification and characterization of membrane-bound semicarbazide-sensitive amine oxidase (SSAO) from bovine lung. *Biochem.J.* **331**:69-78.

Salmi M, Kalimo K, and Jalkanen S (1993) Induction and function of vascular adhesion protein-1 at sites of inflammation. *J.Exp.Med.* **178**:2255-2260.

Salter-Cid LM, Wang E, O'rourke AM, Miller A, Gao H, Huang L, Garcia A, and Linnik MD (2005) Anti-inflammatory effects of inhibiting the amine oxidase activity of SSAO. *J.Pharmacol.Exp.Ther.* **315**:553-562.

Santizo RA, Anderson S, Ye S, Koenig HM, and Pelligrino DA (2000a) Effects of estrogen on leukocyte adhesion after transient forebrain ischemia. *Stroke* **31**:2231-2235.

Santizo RA, Koenig HM, and Pelligrino DA (2000b) Estrogen and leukocyte adhesion following transient forebrain ischemia in rats. *Stroke* **31**:2231-2235.

Santizo RA, Xu HL, Ye S, Baughman VL, and Pelligrino DA (2002) Loss of benefit from estrogen replacement therapy in diabetic ovariectomized female rats subjected to transient forebrain ischemia. *Brain Res.* **956**:86-95.

Schmued LC and Hopkins KJ (2000) Fluoro-Jade B: a high affinity fluorescent marker for the localization of neuronal degeneration. *Brain Res.* **874**:123-130.

Siman R, Zhang C, Roberts VL, Pitts-Kiefer A, and Neumar RW (2005) Novel surrogate markers for acute brain damage: cerebrospinal fluid levels correlate with severity of ischemic neurodegeneration in the rat. *J.Cereb.Blood Flow Metab* **25**:1433-1444.

Stolen CM, Marttila-Ichihara F, Koskinen K, Yegutkin GG, Turja R, Bono P, Skurnik M, Hanninen A, Jalkanen S, and Salmi M (2005) Absence of the endothelial oxidase AOC3 leads to abnormal leukocyte traffic in vivo. *Immunity.* **22**:105-115.

Sughrue ME, Mehra A, Connolly ES, Jr., and D'Ambrosio AL (2004) Anti-adhesion molecule strategies as potential neuroprotective agents in cerebral ischemia: a critical review of the literature. *Inflamm.Res.* **53**:497-508.

Wang J, Liu S, Fu Y, Wang JH, and Lu Y (2003) Cdk5 activation induces hippocampal CA1 cell death by directly phosphorylating NMDA receptors. *Nat.Neurosci.* **6**:1039-1047.

Wang Q, Santizo R, Baughman VL, and Pelligrino DA (1999) Estrogen provides neuroprotection in transient forebrain ischemia through perfusion-independent mechanisms in rats. *Stroke* **30**:630-637.

Wang X, Tsuji K, Lee SR, Ning M, Furie KL, Buchan AM, and Lo EH (2004) Mechanisms of hemorrhagic transformation after tissue plasminogen activator reperfusion therapy for ischemic stroke. *Stroke* **35**:2726-2730.

Xu HL, Baughman VL, and Pelligrino DA (2004) Estrogen replacement treatment in diabetic ovariectomized female rats potentiates postischemic leukocyte adhesion in cerebral venules. *Stroke* **35**:1974-1978.

Xu HL, Galea E, Santizo RA, Baughman VL, and Pelligrino DA (2001) The key role of caveolin-1 in estrogen-mediated regulation of endothelial nitric oxide synthase function in cerebral arterioles *in vivo*. *J.Cereb.Blood Flow Metab.* **21**:907-913.

Yong Y, Xie HJ, Zhang YF, Yang QD, Liao DF, Yang HL, Yan PK, and Liu ZJ (2005) 17beta-estradiol potentiates ischemia-reperfusion injury in diabetic ovariectomized female rats. *Brain Res.* **1054**:192-199.

Yu PH, Wright S, Fan EH, Lun ZR, and Gubisne-Harberle D (2003) Physiological and pathological implications of semicarbazide-sensitive amine oxidase. *Biochim.Biophys.Acta* **1647**:193-199.

Footnotes:

This work was supported by DK65629 and HL52594.

Legends for Figures

Figure 1: Post-ischemic leukocyte presence at 2-10h reperfusion in saline-treated rats (n=6), rats treated with LJP-1207 at the onset of reperfusion (LJP-0h, n=4) or at 6h reperfusion (LJP-6h, n=8), and neutropenic rats (n=7). The results in panel **A** were calculated by first measuring the fraction of the field of view area occupied by pial venules. Second, the fraction of the field of view area occupied by leukocytes was measured. Thus, pial venular "leukocyte adhesion" was calculated by dividing the second value by the first value (multiplied by 100%). In the absence of any rhodamine 6G fluorescence clearly outside the outside margins of the venules, it was assumed that diapedesis had not occurred. For the results presented in panel **B**, the leukocyte fraction includes all leukocytes present within the field of view, irrespective of whether the leukocytes are or are not in contact with a venule. In this case, "total leukocyte presence" is calculated by dividing the leukocyte fraction by the venular fraction within the same field of view (times 100%). An "index of infiltration" in individual rats was calculated as the difference between total leukocyte presence (panel **B**) and adherent leukocytes (panel **A**). Those results are provided in panel **C**. Only the time points where the mean value of this calculation was >0 are reported. Thus, panel **C** contains data only from the saline-treated and LJP-6h groups, at reperfusion times of 6, 8, and 10h. Values are means ± SD. *$p<0.05$ vs LJP-0h; $^{\S}p<0.05$ vs neutropenia; $^{\dagger}p<0.05$ vs LJP-6h.

Figure 2: Representative images of pial venular leukocyte adhesion captured at 4, 6 and 10h reperfusion in the 4 groups of animals evaluated in the present study.

Figure 3: Myeloperoxidase (MPO) immunohistochemistry (at 10-12h reperfusion), depicting neutrophil presence in the cerebral cortex (A-E) of saline-treated (A-C), 0h LJP-1207-treated (D), and 6h LJP-1207-treated (E) rats; and in the striatum (F) and thalamus (G) of saline-treated controls. Note the presence of extravascular neutrophils in the cortex of the controls; while, in the 0h and 6h LJP-1207-treated rats, MPO immunoreactivity remained associated with blood vessels. Note also the limited neutrophil presence in the ischemic striatum and thalamus. Scale bars are 100 μm (panel A) or 50 μm (panels B-F).

Figure 4: Neurologic outcome scores for all rats evaluated in the present study. The scoring system was weighted toward assessments of motor function. The saline-treated control data represents the results obtained in all control groups, irrespective of whether the data was gathered along with the LJP-treated groups or the anti-PMNL group. The control measurements were treated in this way since no differences were seen when comparing results from the different control groups. The horizontal bars depict the median values. *$p<0.05$ vs saline-treated control.

Figure 5: Quantitative neuropathology in saline-treated control rats (n=10); rats treated with LJP-1207 at the onset of reperfusion (LJP-0h [n=7]) or 6h reperfusion (LJP-6h [n=6]); and neutropenic rats (n=5). The numbers of Fluoro-Jade B (FJ)-positive cells (represents degenerating neurons) in the 4 brain regions exhibiting FJ reactivity were counted. Values are means ± SD. *$p<0.05$ vs saline-treated control; $^{\dagger}p<0.05$ vs LJP-1207 (0h reperf.).

Figure 6: Representative photomicrograph showing Fluoro-Jade-positive neurons in the cortex (A-C) and striatum (D-F) in saline-treated control rats (A, D) and in rats treated with LJP-1207 at the onset (LJP-1207-0h; B, E) or at 6h (LJP-1207-6h; C, F) of reperfusion. Horizontal bar=100μm. Inset depicts higher magnification view of the area outlined.

Figure 7: Representative photomicrographs showing Fluoro-Jade-positive neurons in the thalamus (A-C) and in the CA4 (hilar) region of the hippocampus (D-F) in saline-treated control rats (A, D) and in rats treated at the onset (LJP-1207-0h; B, E) or at 6h (LJP-1207-6h; C, F) of reperfusion. Horizontal bar=100μm. Inset depicts higher magnification view of the area outlined.

Figure 8: Comparison of Fluoro-Jade (A, C, E) and H&E (B, D, F) staining in 7 μm sections obtained from the ischemic hemisphere in saline-treated control (A, B, E, F) or 6h LJP-1207-treated (C, D) rats. Views are at the level of the dentate and hilar regions of the hippocampus (A-D) or the cerebral cortex (E, F). Scale bar = 100μm. See text.

JPET Fast Forward. Published on December 8, 2005 as DOI: 10.1124/jpet.105.096958
This article has not been copyedited and formatted. The final version may differ from this version.

TABLE 1. LJP-1207 selectivity screen.

Enzyme	Source	IC_{50}
VAP-1/SSAO	rat lung	0.035
MAO-A	human recombinant	225
MAO-B	human recombinant	100

IC_{50} values are expressed in μM units.

Figure 1

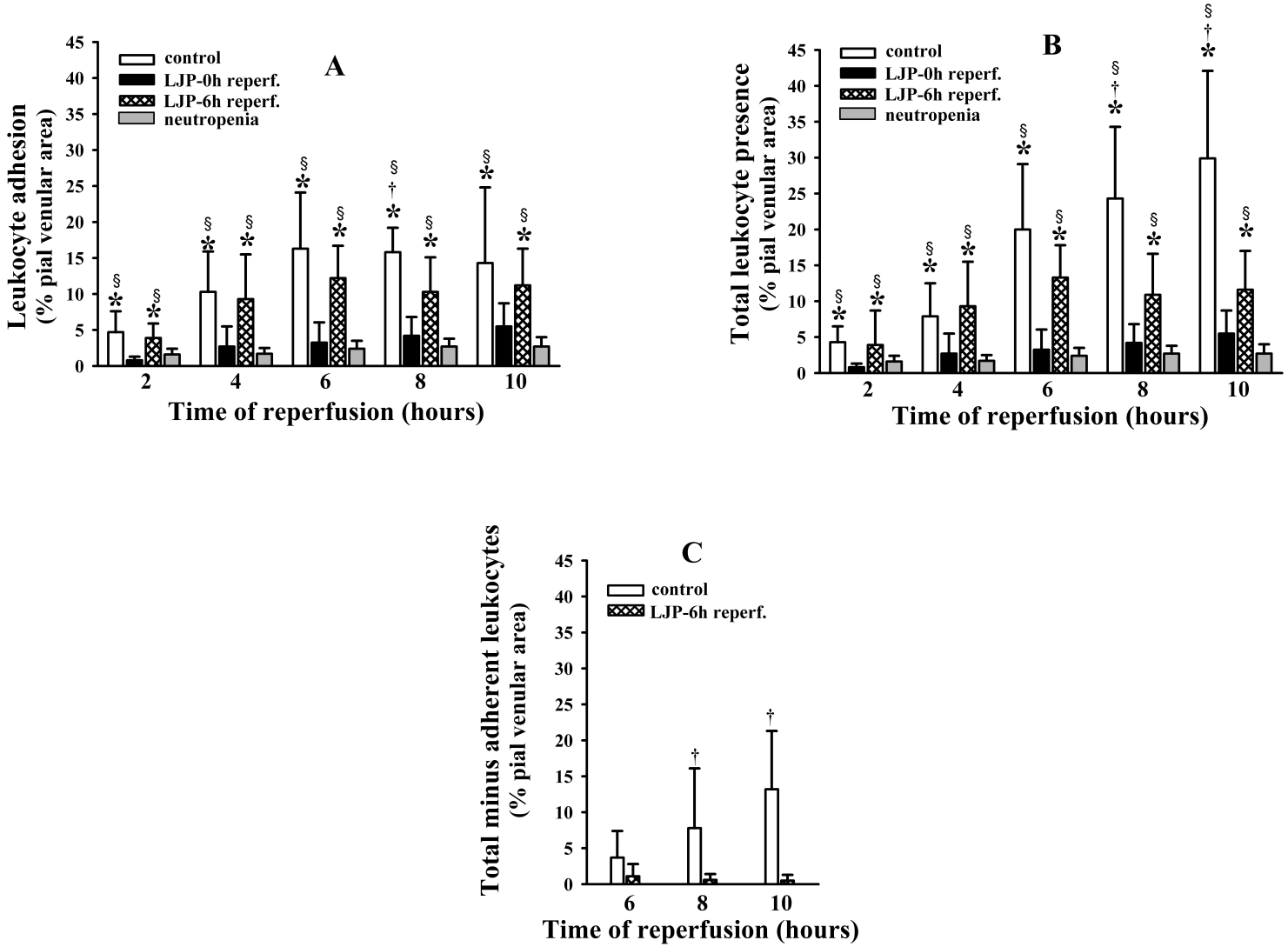

Figure 2

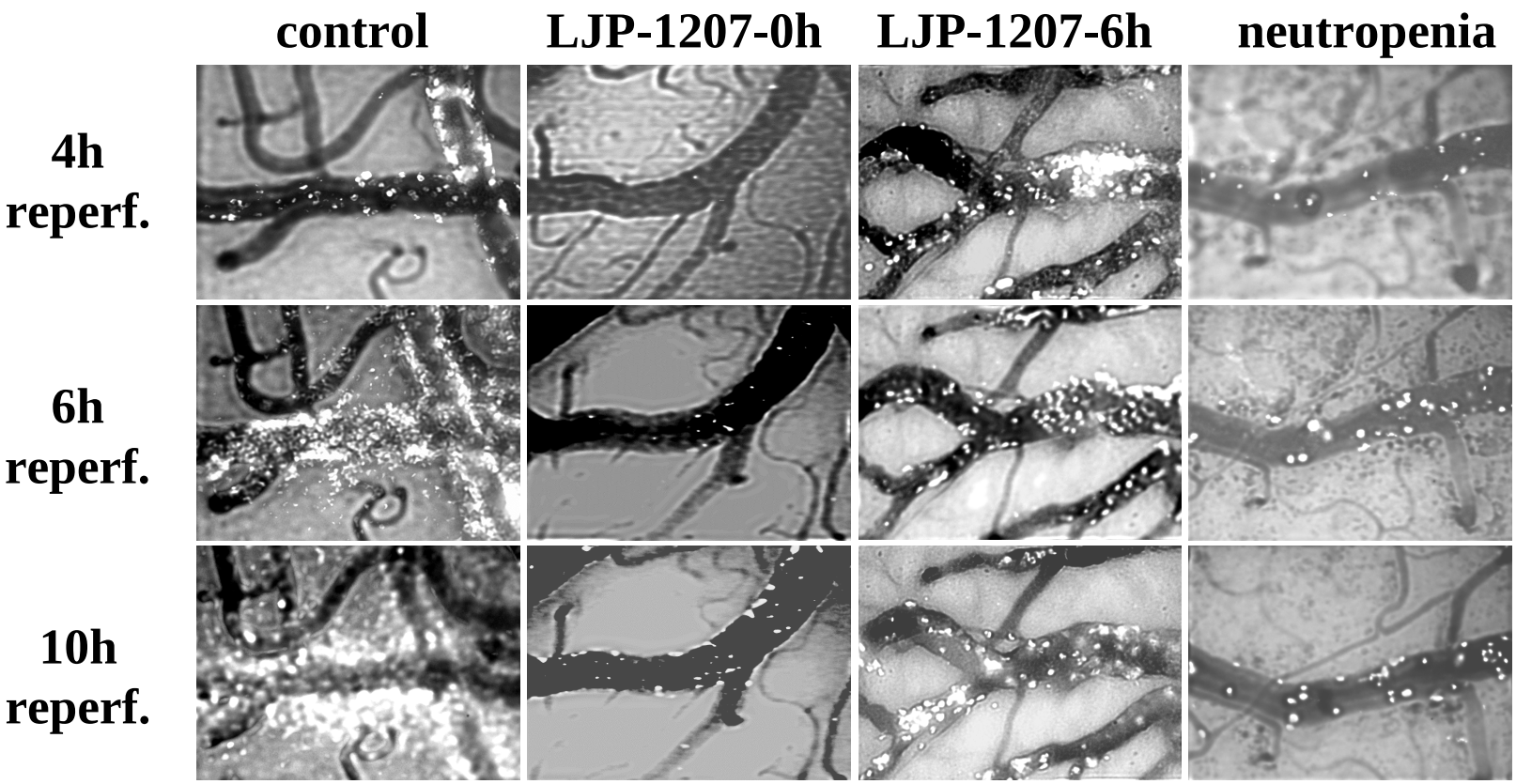

JPET Fast Forward. Published on December 8, 2005 as DOI: 10.1124/jpet.105.096958
This article has not been copyedited and formatted. The final version may differ from this version.

Figure 3

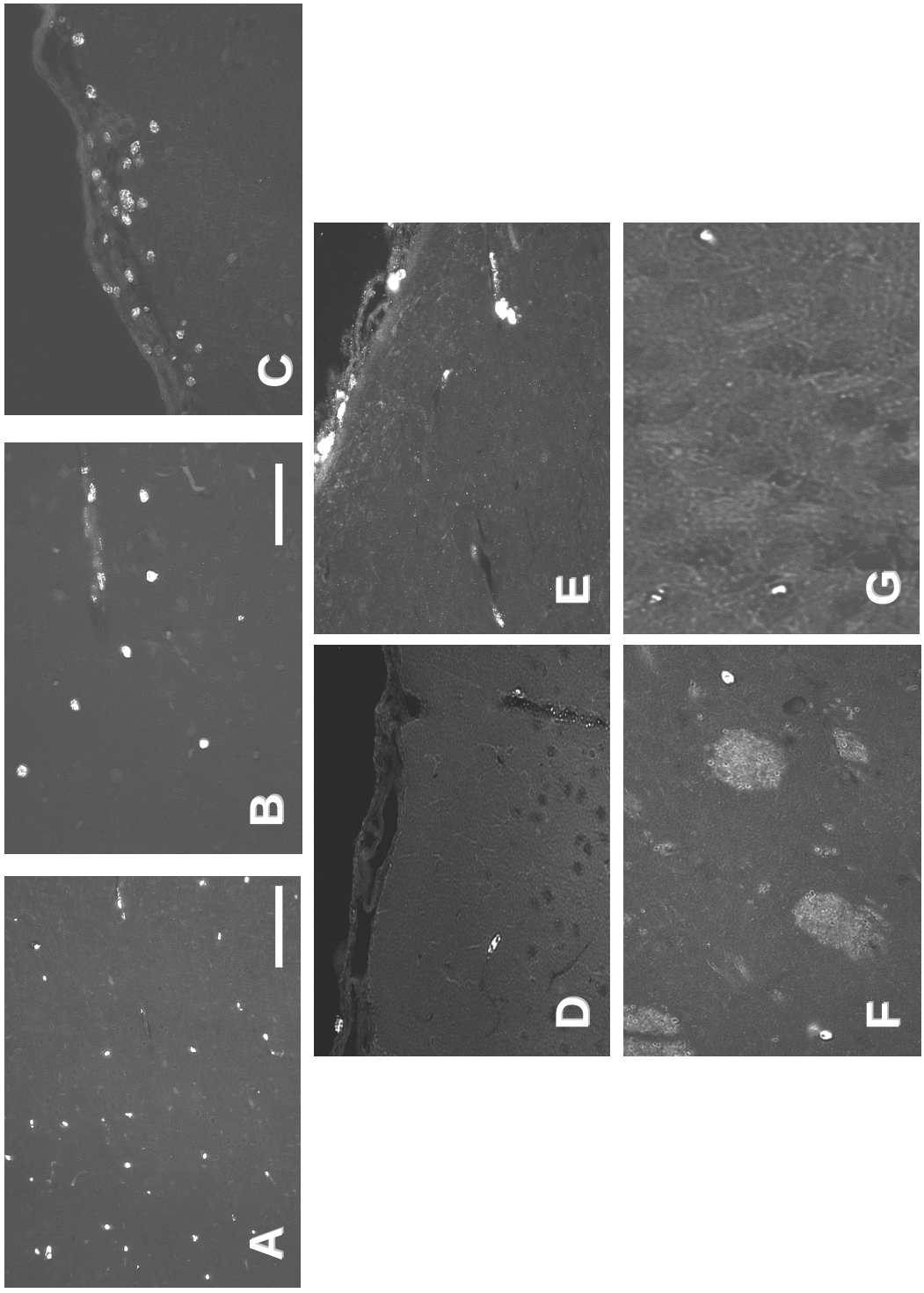

Figure 4.

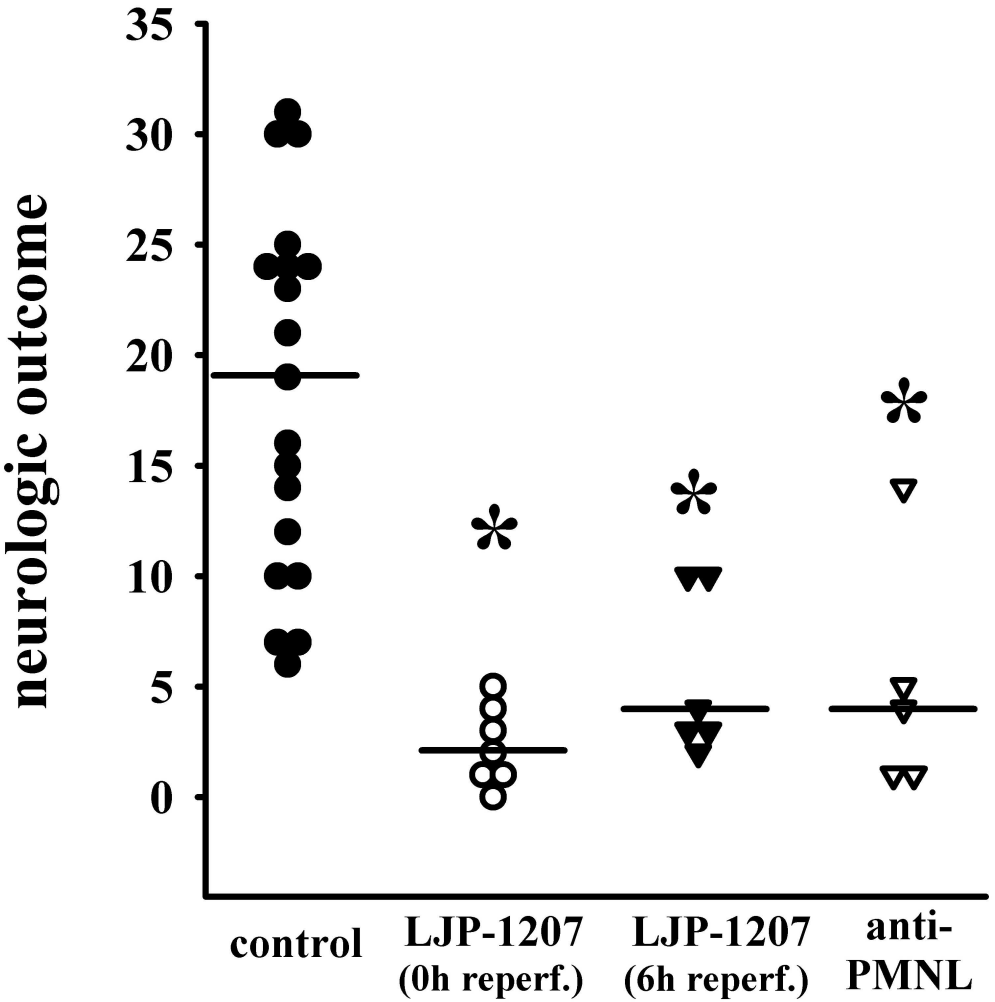

Figure 5.

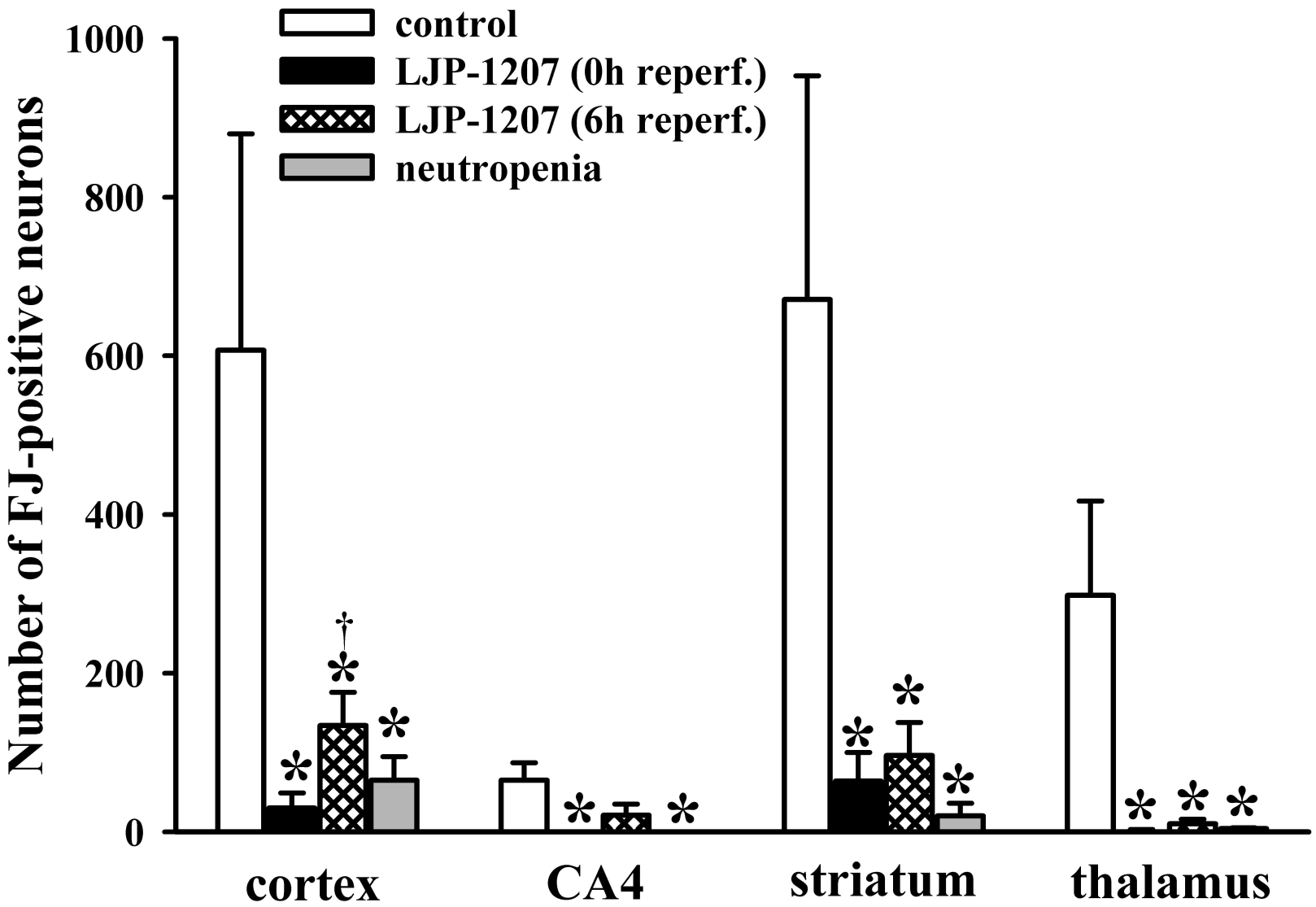

Figure 6.

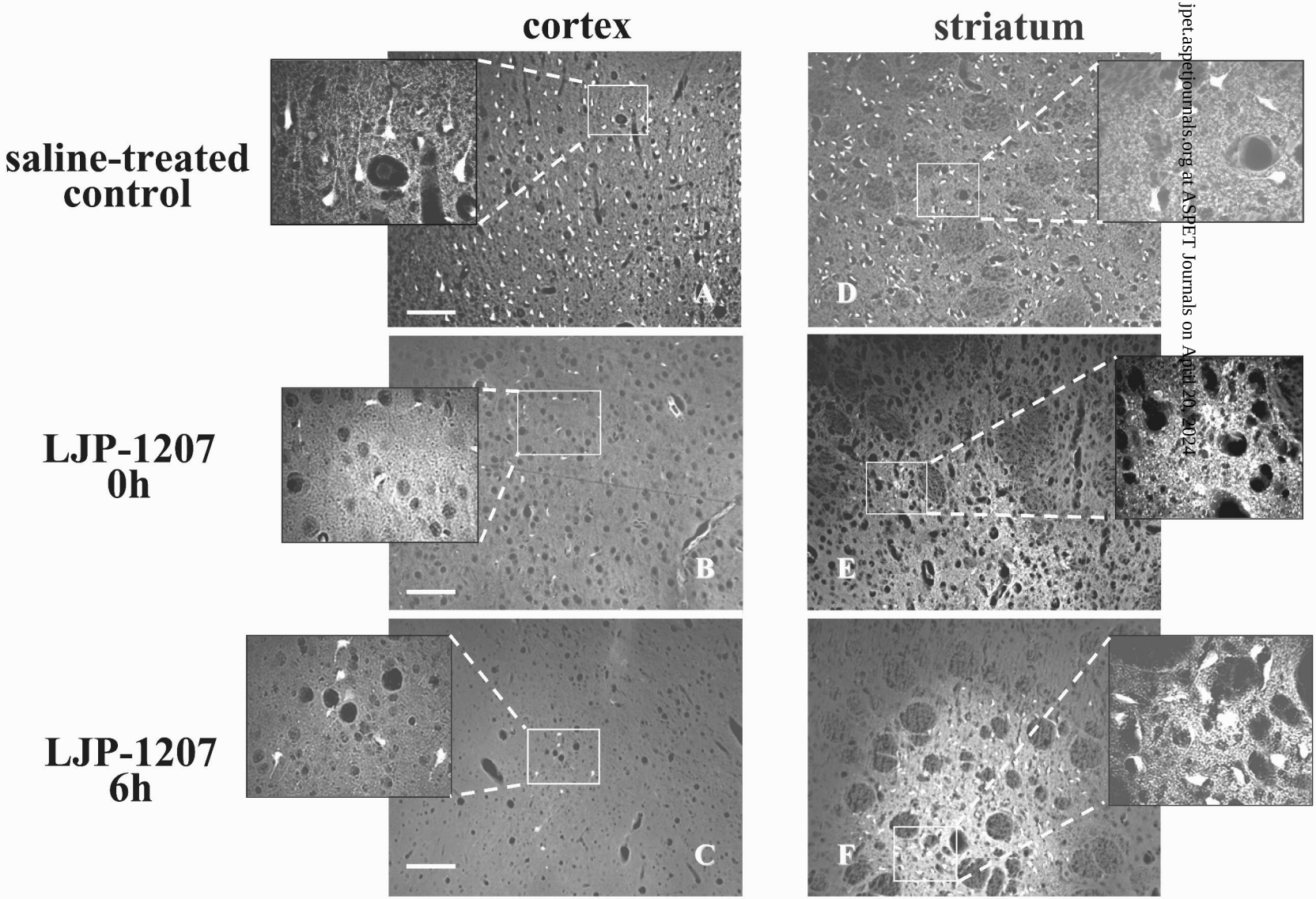

Figure 7.

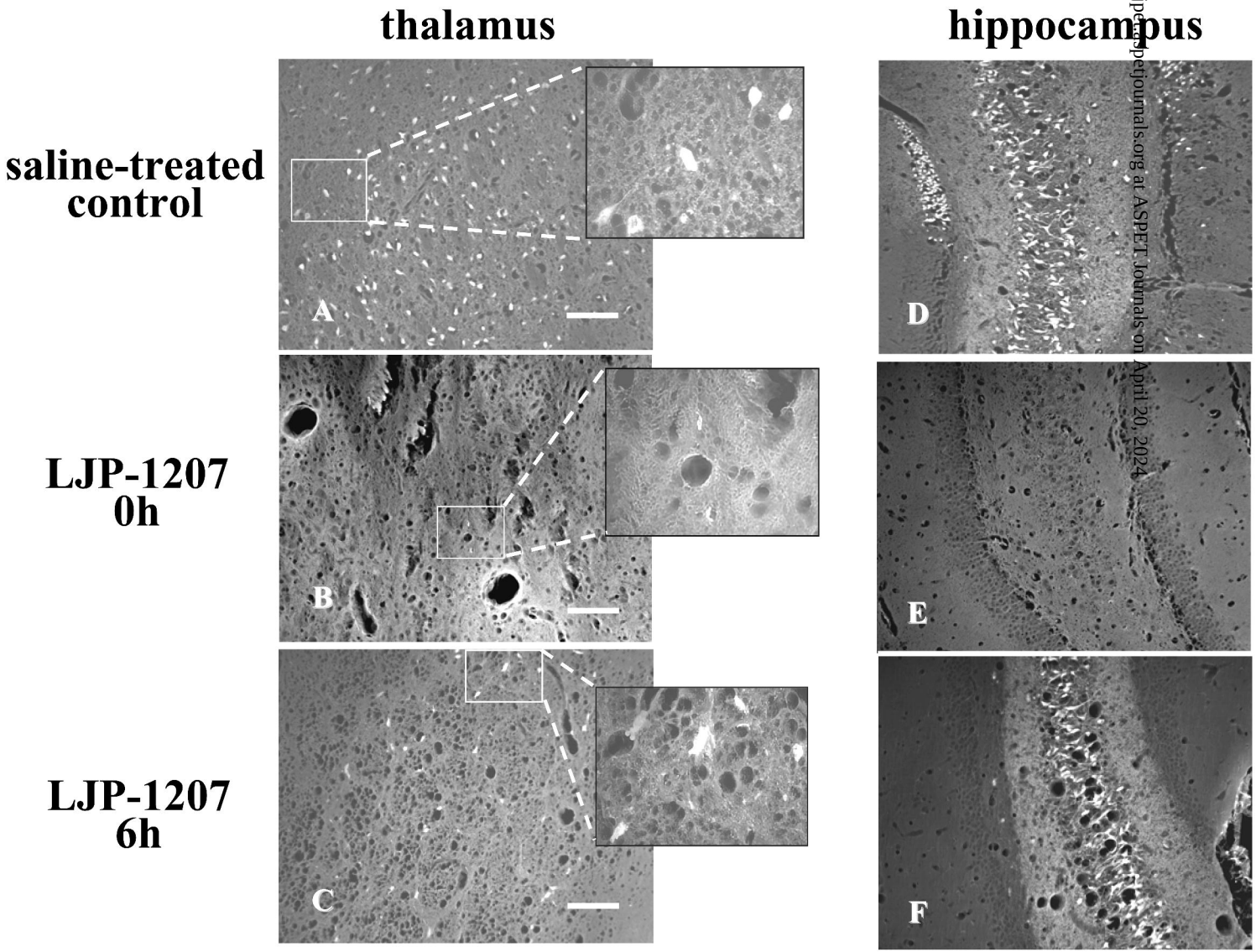

Figure 8.